SIMULATION OF A SHELL-AND-TUBE VERTICAL EVAPORATOR OF UPWARD BOILING FLUID FLOW COOLING A NANOFLUID

Yipsy Roque Benito, gipsyrb@aluno.puc-rio.br
José Alberto Reis Parise, parise@puc-rio.br
PUC-Rio, Rua Marquês de São Vicente 225, Gávea, Rio de Janeiro, RJ, Brasil
Jesús Betancourt Mena, betancourt@uclv.edu.cu
Center for Energy Technologies and Environmental Assessments (CEETA). Universidad Central Marta Abreu de Las Villas (UCLV). C. Camajuani, K5,5 Santa Clara, VC, CP 54830, Cuba.
José Viriato Coelho Vargas, jvargas@demec.uf
UFPR,Centro Politécnico (Campus II), Bairro Jardim das Américas, Curitiba, PR, Brasil

Abstract.
A mathematical model of the evaporator of an ammonia-water absorption refrigeration system, with a nanofluid as the heat transfer fluid is presented in this paper. The evaporator type is that of a vertical shell-and-tube heat exchanger, operated at steady state conditions, with upward refrigerant flow through the tubes whilst the cooled nanofluid flows through the shell. A local analysis for the refrigerant to inner tube wall heat exchage was applied to both distinct regions considered, the two-phase region and the superheated vapor region. The application of energy balance and heat transfer rate equations on each heat exchanger element resulted in a system of nonlinear equations which is only tractable through numerical methods. A Fortran code was developed to obtain the solution of such a model and comparisons of the performance of the evaporator were made on the basis of considering different nanofluid párticles with water as the base fluid and just water as the cooled fluid.

***Key words**: Shell-and-tube evaporator, nanofluid applications.*

1. INTRODUCTION

The mathematical simulation of a system consists of a set of equations that represents the physical model of a problem post in reality. The use of the mathematical simulation is a common practice in engineering for projecting, optimizing and diagnosing different engineered systems and system components.

The object of the study is a vertical shell-and-tube heat exchanger with upward flow of vaporizing ammonia inside the tubes and a nanofluid cooled on the shell side, as illustrated in Fig. 1.

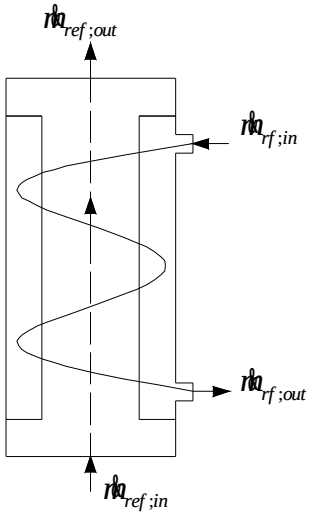

Figure 1. Schematic representation of the evaporator

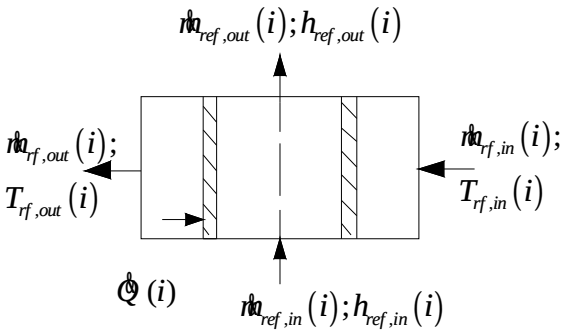

Figure 2. Scheme of the i-th heat exchanger element

The use of nanofluids as thermal fluids in different applications is steadily increasing since the suspension of nanoparticles of high thermal conductivity enhances their heat transfer characteristics. The nanofluids inhibit heat exchange capacities higher than that of the conventional fluids such as water, ethylene glycol or oil (Yu *et al*, 2008). In this regard nanofluids are envisioned as the next generation of heat transfer fluids in order to attain an improved performance of heat exchanger when compared to their operation with conventional heat transfer fluids.

The mathematical model of the heat exchanger under study is described in the next section.

2. MODEL

In the present study the heat exchanger is divided into "small" similar elements to account for the local variation of the heat transfer coefficient with the ammonia vapor quality over the heat transfer area exposed to the two-phase flow pattern. Fig. 2 shows the geometry of the element, and also the mass and energy flows.

Each element is treated as a small heat exchanger in which the energy balance equations may be applied as well as the heat transfer rate equation. A lumped parameters model and local properties of the fluids are considered within each element. The heat exchange is analyzed by the thermal effectiveness method, *e-NTU.*

2.1 Simplifying Hypotheses.

The following hypotheses were taken into consideration for the evaporator:

i) The water as the absorbent does not vaporizes in the generator; therefore only pure ammonia as the refrigerant flows from the evaporator to the condenser.
ii) The heat exchanger operates at steady state conditions.
iii) Heat losses to the environment are negligible (The heat exchanger is considered to be adiabatic).
iv) The temperature profile throughout each cross section of either heat transfer fluid sides is uniform.
v) The heat transfer area is evenly distributed on each fluid side.
vi) The heat flux is uniform over each heat exchanger element.
vii) The convective heat transfer coefficient for the flow through the tubes is constant over each heat exchanger element.
viii) For two-phase refrigerant flow, vapor quality is considered constant over each heat exchanger element.
ix) The convective heat transfer coefficient on the cooled fluid side is constant along the heat exchanger.
x) The nanofluids here studied are considered as homogeneous fluids with perfectly spherical particles.
xi) The thermophysical properties of nanofluids are determined at the mean temperature of the base fluid.

2.2 Heat Transfer and Balance Equations.

For each heat exchanger element heat balance may be written as follows:

- On the cooled fluid side:

$$\dot{Q}_{EVA} = \dot{m}_{rf;EVA} c_{p;rf} \left(T_{rf;in} - T_{rf;out} \right) \tag{1}$$

- On the refrigerant side:

$$\dot{Q}_{EVA} = \dot{m}_{ref;EVA} c_{p;ref} \left(h_{ref;out} - h_{ref;in} \right) \tag{2}$$

The heat transfer rate may be defined in terms of the thermal effectiveness of the evaporator resulting in the form of the heat transfer equation (Eq 3).

$$\dot{Q}_{EVA} = e_{EVA} C_{\min} \left(T_{rf;in} - T_{ref,in} \right) \tag{3}$$

The evaporator thermal effectiveness may be expressed as that of any heat exchanger with phase change for the evaporator section exposed to the vaporizing ammonia:

$$e_{EVA} = 1 - \exp\left(- \frac{UA_{EVA}}{\dot{m}_{rf;EVA} c_{p,rf}} \right) \tag{4}$$

The thermal effectiveness formula for the section of evaporator exposed to superheated refrigerant vapor is that of a tube and shell heat exchanger with prevailing counterflow and sensible heat exchange only, and with one pass through the shell and one pass in the tubes coincides with that of pure counterflow heat exchanger effectiveness. (Baclic, 1997).

$$e_{EVA} = \frac{1 - \exp\left[-NTU\left(1 - C_r\right)\right]}{1 - C_r \exp\left[-NTU\left(1 - C_r\right)\right]} \tag{5}$$

where:

$$C_r = \frac{C_{\min}}{C_{\max}} = \frac{\left(\dot{m} c_p\right)_{\min}}{\left(\dot{m} c_p\right)_{\max}} \tag{6}$$

$$NTU = \frac{UA}{C_{\min}} \tag{7}$$

The overall heat transfer conductance (UA) is expressed in terms of all individual thermal resistances as in Eq. (8):

$$\frac{1}{UA} = \frac{1}{a_{ref} A_{\text{int}}} + \frac{d_{tub}}{k_{tub}} + \frac{1}{a_{rf} A_{ext}} \tag{8}$$

where: $A_{\text{int}} = p\, D_{t;\text{int}} L_t N$ (9)

$$A_{ext} = p\, D_{t;ext} L_t N \tag{10}$$

and d_{tub} is the tube wall thickness, D_t is the tube inner or outer diameter, N is the number of tubes of the evaporator and L_t is the length of each heat exchanger element.

2.3 Convection heat transfer coefficient for the flow through the tubes, a_{ref}

As refrigerant vaporizes within the tubes, two regions may be identified, namely the two-phase region wherein the vapor and the liquid phase coexist and the superheated vapor region.

2.3.1 Two-phase region

In case of two-phase flow in tubes, both the convective heat transfer coefficient and the pressure gradient vary significantly along the tube axes, depending on the liquid/vapor phase's distribution.

The local two-phase flow boiling heat transfer coefficient for evaporation inside the tubes, a_{tp}, is determined according to Steiner and Taborek asymptotic model thoroughly described by Collier and Thome (1994).

2.3.1.1 Boiling flow model

The boiling heat transfer coefficient is calculated by the Steiner and Taborek asymptotic model with exponent equal 3 which applies for vertical ducts.

$$a_{tp} = \left[\left(a_{Lt} F_{tp}\right)^3 + \left(a_{nb,o} F_{nb}\right)^3\right]^{1/3} \tag{11}$$

Parameters in Eq. (11) are as follows:

- a_{Lt}, Forced convective coefficient for the whole flow considering as though it were entirely a liquid flow and it is calculated through Gnielinski´s correlation;
- F_{tp}, two-phase multiplier that accounts for the increase in convective heat transfer of liquid phase resulting from the higher flow velocity of a two-phase flow when compared to a single-phase flow;

- $a_{nb,o}$, local 'normalized' nucleate pool boiling coefficient which is determined for the reference value of heat flux q_o, at the reduced pressure p_r equal to 0.1;
- F_{nb} nucleate boiling correlation factor.

Since the Steiner and Taborek´s method does not predict the behavior of the heat transfer coefficient for vapor qualities beyond x_{crit} (critical value), a method like that proposed by Shah (1987) was necessary to calculate the aforementioned heat transfer coefficient.

2.3.1.2 Model for the p*ost-dryout* region

Groeneveld (1973) gives a heat transfer correlation that applies well to the "post-dryout" region; such a correlation may be expressed as:

$$Nu_V = a\left\{\frac{GDt_{\text{int}}}{m_V}\left[x+\frac{r_V}{r_L}(1-x)\right]\right\}^b \text{Pr}_V^c\, Y^d \tag{12}$$

where $Y = 1-0.1\left[\left(\frac{r_L}{r_V}-1\right)(1-x)\right]^{0.4}$ (13)

and the constants a, b, c, d are described in Collier and Thome (1994).

2.3.2 Superheated vapor region

The convective heat transfer coefficient for the superheated vapor region is determined by using the Dittus-Bolter correlation:

$$Nu_V = 0.023\,\text{Re}_V^{0.8}\,\text{Pr}_V^{0.4} \tag{14}$$

2.4 Convective heat transfer calculation on the shell side., a_{rf}

The Bell-Delaware´s method (Rohsenow *et al*, 1998) was used to determine the convective heat transfer coefficient on the shell side a_{rf} .In so doing a correction factor to the ideal heat transfer coefficient $a_{rf,ideal}$ is introduced in order to account for baffles effects on heat transfer and fluid flow within the heat exchanger such as distorted flow patterns, bypass and leakage.

$$a_{rf} = a_{rf,ideal} \times J \tag{14}$$

The correction factor, J , is, in turn, defined as a product of five factors that accounts for recirculation and leakage effects.

The coefficient $a_{rf,ideal}$ is determined for a pure counterflow tube bundle according to the expression:

$$a_{rf,ideal} = j_{ideal} \times c_{p,cf} \times Gc_{rf} \times \text{Pr}_{rf}^{-2/3} \times \left(\frac{(m_{cf})_s}{(m_{cf})_{wall}}\right)^{0.14} \tag{15}$$

The Colburn j_{ideal} (ideal) for a bundle of tubes is determined by the equation (16):

$$j_{ideal} = a_1 \times \left(1.33 \times \frac{D_{t,ext}}{Pt}\right)^a \times \text{Re}^{a_2} \tag{16}$$

$$a = \frac{a_3}{1+0.14\times \text{Re}^{a_4}} \tag{17}$$

where a_1, a_2, a_3, a_4 depend on heat exchanger tube arrangement and the Reynolds number (Thome, 2009)

The determination of the convective heat transfer coefficient for a cooling process of a nanofluid is carried out by calculating the thermophysical properties of the fluid through a single-phase model like those proposed by Xuan and Li (2003), Heris et al (2006) and Pak and Cho (1998). In these models, the fluid and the suspended nanoparticles are considered a homogeneous fluid.

Thermophysical properties of nanofluids.

The heat transfer coefficient of a nanofluid depends on the thermophysical properties of both base fluid and the nanoparticles. In this work, the properties of metallic oxides are considered constant and equal to those provided in Velagapudi *et al*, 2008, in case of the water properties used as the base fluid, the properties were estimated by means of the Refprop 7.0 Code subroutine (Lemmon *et al*, 2002)

Table 1 Properties of the nanoparticles (Velagapudi *et al*, 2008)

		Al2O3	CuO	TiO2
$c_{p,np}$	kJ/kg K	0,765	0.535	0,686
r_{np}	kJ/m3	3790	6500	4250
k_{np}	kW/m K	0,040	0,020	0,0895
u_{np}	m2/s	1317	57,45	30,07

According to the physical principle of mixtures rule, the effective density, r_{nf}, and the effective specific heat, $c_{p,nf}$, may be computed as functions of volumetric concentration of nanoparticles, j_{np}, as follows:

$$r_{nf} = \left(1 - j_{np}\right) r_{bf} + j_{np} r_{np} \tag{18}$$

$$c_{p,nf} = \frac{\left(1 - j_{np}\right)\left(r c_p\right)_{bf} + j_{np}\left(r c_p\right)_{np}}{r_{nf}} \tag{19}$$

Jang and Choi (2004) developed a dynamic model to calculate the thermal conductivity of nanofluids, k_{nf}, that accounts for the Brownian motion of nanoparticles and it is expressed as:

$$k_{nf} = k_{bf}\left(1 - j_{np}\right) + b\,k_{np} j_{np} + 3C_l \frac{d_{bf}}{d_{np}} k_{bf}\,\mathrm{Re}_{d,np}^2\,\mathrm{Pr} \tag{20}$$

where k_{nf} is the conductivity of the base fluid, b is a constant relative to the Kapitza resistance, C_l is an empirical constant of proportionality, d_{bf} is the diameter of molecules of the base fluid and d_{np} is the diameter of the nanoparticle.

The Reynolds number depends on the kinetic viscosity of the base fluid and the random motion velocity of the nanoparticles, the latest being described in details by Jang and Choi (2006).

$$\mathrm{Re}_{d,np} = \frac{\bar{C}_{RM} d_{np}}{u_{bf}} \tag{21}$$

Einstein´s equation is used to calculate the dynamic viscosity of the fluids; a validation was made by Heris *et al* (2006) for AL_2O_3+H_2O and CuO+H_2O:

$$m_{nf} = m_{bf}(2.5 j_{np} + 1) \tag{22}$$

Pak and Cho (1998) presented the following empirical correlation for TiO_2+H_2O.

$$m_{nf} = m_f (108 j_{np}^2 + 5,45 j_{np} + 1) \tag{23}$$

Reynolds and Prandtl numbers of nanofluids are defined according to Heris *et al* (2006) by the expressions (24) and (25) respectively:

$$\mathrm{Re}_{nf} = \frac{r_{nf} \bar{u}_{nf} D_{t,ext}}{m_{nf}} \tag{24}$$

$$\mathrm{Pr}_{nf} = \frac{m_{nf} c_{p;nf}}{k_{nf}} \tag{25}$$

where $\bar{u}_{nf}$, is the velocity of the nanofluid entering the heat exchanger.

3 NUMERICAL SOLUTION

3.1 Metodology

An approximate outlet temperature of the cooled nanofluid is assumed, and then the heat transfer and energy balance equations (Eq 1-3) are applied to each heat exchanger elements along the refrigerant flow direction from the refrigerant inlet to its outlet. Heat exchanger geometry, refrigerant mass flow rate and the properties of both refrigerant and cooled fluid are entry data to the model. The temperature of the cooled fluid is calculated accompanying the refrigerant path from its inlet to its outlet and then this calculated value is compared to the actual temperature value of the cooled fluid at the evaporator inlet; a correction is then made until the convergence criterion is satisfied. Figure 3 illustrates the basic algorithm of the model solution.

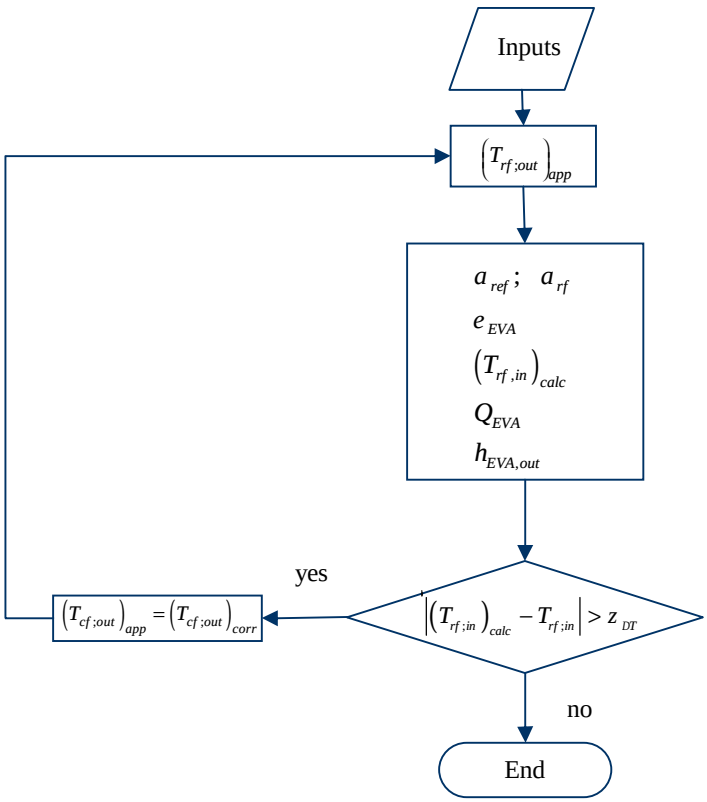

Figure 3. Block diagram containing basic algorithm of solution

3.2 Simulation

The mathematical model described above, was implemented in a FORTRAN computational code and the performance of the evaporator was evaluated for water as the cooled fluid and three different nanofluids with water as the base fluid. Conditions such as particle diameter, base temperature fluid and volumetric concentration of nanoparticles were maintained constant for the evaluation

3.3 Entry data.

Geometry	
Number of tubes	76
Length of tubes	0.65 m
Bundle of tubes arrangement	30°
Outer diameter (3/8")	9.525 mm
Tube wall thickness	1.245 mm
Refrigerant	
Mass flow rate	0.03 kg/s
Inlet pressure	2500 kPa
Inlet temperature	267 K
Cooled fluid	
Inlet temperature.	294 K
Mass flow rate	0.6 – 0.9 kg/s
Nanoparticles concentration	0.02
Nanoparticles diameter	20 nm

4. RESULTS

The proposed mathematical model was run to obtain the simulation results as a function of the Péclet number of the cooled fluid flow.

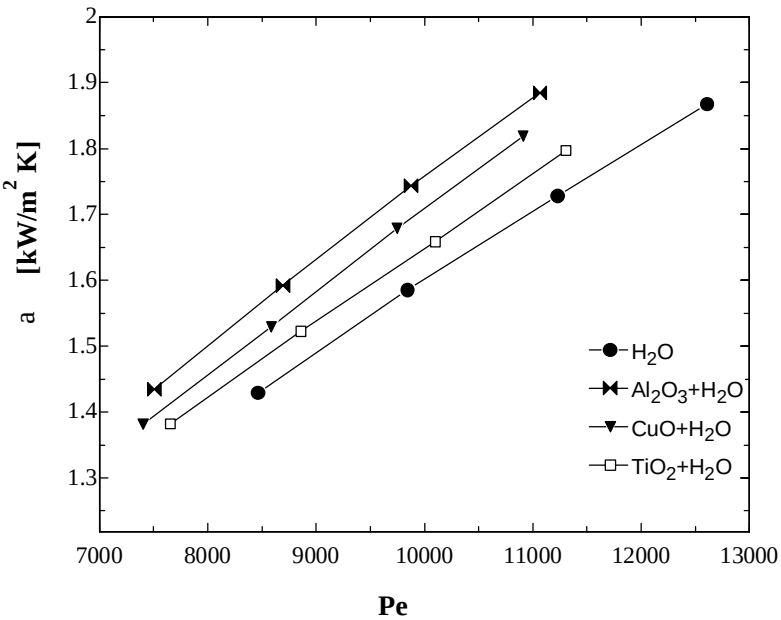

Figure 4. Convective heat transfer coefficient on the shell side, $j = 2,0\%$ $d_p = 20nm$

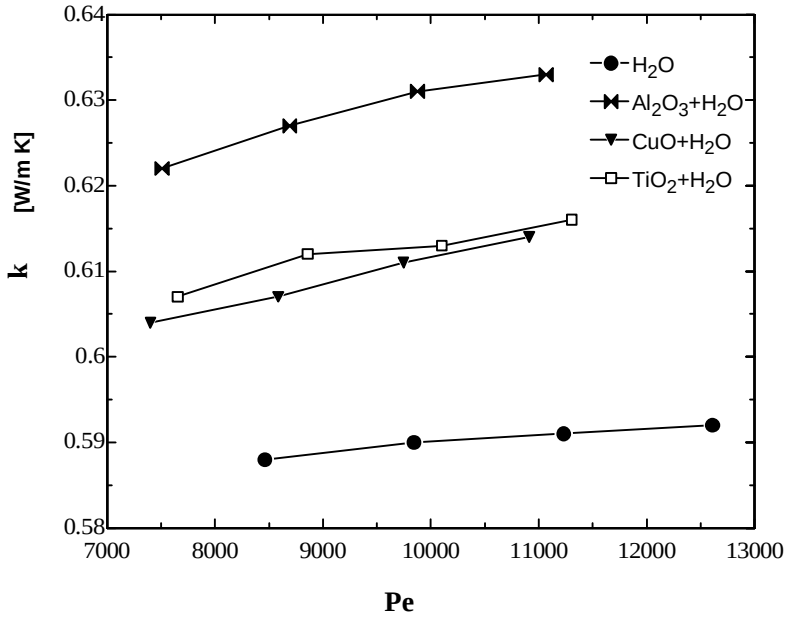

Figure 5. Thermal conductivity of the cooled fluid flow. $j = 2,0\%$ $d_p = 20nm$

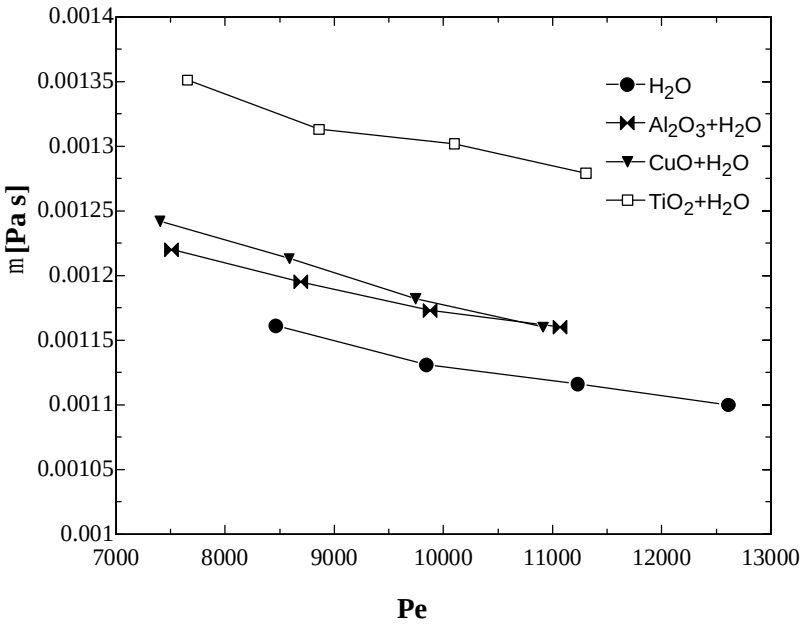

Figure 6. Dynamic viscosity of the cooled fluid flow. $j = 2,0\%$ $d_p = 20nm$

5. CONCLUSIONS

The figures 4 through 6 indicate an expected trend of increasing thermal conductivity and dynamic viscosity of water-based nanofluid when compared to water. The convective heat transfer coefficient on the cooled fluid side also shows a better performance of the evaporator when operated with nanofluids instead of pure water.

A great effort has been made during the last years to correctly understand the heat and momentum transfers in nanofluids. Very recently, some attention has been paid to nanofluid applications in diverse areas of engineering, being the present paper an initial contribution for the study of the nanofluid application to heat exchangers.

6. ACKNOWLEDGEMENT

Thanks are due to CNPq, FAPERJ and CAPES, Brazilian research funding agencies, for financial support.

7. REFERENCES

Baclic, B. S., 1997, "1-(2N-1) shell-and-tube exchanger effectiveness: explicit equations", Heat and Mass Transfer Volume 33, Numbers 1-2, pp 163-165

Collier, J. G., Thome, J. R., 1994, "Convective Boiling and Condensation". Oxford University Press, Oxford.

Heris, S. Z., Etemad, S. Gh. and Esfahany, M. N., 2006, "Experimental Investigation of Oxide Nanofluids", Laminar Flow Convective Heat Transfer. International Communications in Heat and Mass Transfer 33: pp 529-535

Jang, S. P., and S. U. S. Choi (2004). Role of Brownian Motion in the Enhanced Thermal Conductivity of Nanofluids. Applied Physics Letters 84: 4316-4318.

Jang, S. P., Choi, S. U.S. (2006) "Cooling performance of a microchannel heat sink with nanofluids". Applied Thermal Engineering 26, 2457–2463

Lemmon E.W., McLinden, M.O., Huber, M.L., NIST Reference Fluid Thermodynamic and Transport Properties -. NIST Std. Database, 2002.

Pak, B. C.; Cho, Y. I. Hydrodynamic and heat transfer study of dispersed fluids with submicron metallic oxide particles. Experimental Heat Transfer [S.I.], v. 11, n. 2, p. 151-170, Apr-Jun 1998.

Pak, B. C.; ChoY. I., (1998), "Hydrodynamic and heat transfer study of dispersed fluids with submicron metallic oxide particles", Experimental Heat Transfer [S.I.], v. 11, n. 2, p. 151-170.

Rohsenow, W. et al., 1998, "Handbook of Heat Transfer", 3rd edition, McGraw-Hill, WW

Shah, M. M. (1987). "Improved general correlation for critical heat flux during upflow in uniformly heated vertical tubes". Heat and Fluid Flow, 8(4), 326-335

Thome, J. R., (2009) "Wolverine Engineering Data Book III". by Wolverine Tube, Inc. Disponível em www.wlv.com

Velagapudi, V. Konijeti, R. K. Aduru, C. S. K. "Empirical correlations to predict thermophysical and heat transfer characteristics of nanofluids". Themal Science, v. 12, pp. 27-37, 2008.

Xuan, Y. Li, Q., 2003, "Investigation on Convective Heat Transfer and Flow Features of Nanofluids". Journal of Heat Transfer , v. 125, n. 1, pp. 151-155.

Yu W.; France; D M. Routbort; J L., Choi. S U. S. "Review and Comparison of Nanofluid Thermal Conductivity and Heat Transfer Enhancements". Heat Transfer Engineering, Volume 29, Issue 5 May 2008 , pages 432 - 460

8. RESPONSIBILITY NOTICE

The authors are the only responsible for the printed material included in this paper.